NETWORKS AND HETEROGENEOUS MEDIA
©American Institute of Mathematical Sciences
Volume **1**, Number **2**, June **2006**

Website: http://AIMsciences.org

pp. **259–274**

ON THE SCALING FROM STATISTICAL TO REPRESENTATIVE VOLUME ELEMENT IN THERMOELASTICITY OF RANDOM MATERIALS

Xiangdong Du

McGill University, Department of Mechanical Engineering
Montreal, QC H3A 2K6, CANADA

Martin Ostoja-Starzewski

University of Illinois at Urbana-Champaign
Department of Mechanical and Industrial Engineering
Urbana, IL 61801, USA

Abstract. Under consideration is the finite-size scaling of effective thermoelastic properties of random microstructures from a Statistical Volume Element (SVE) to a Representative Volume Element (RVE), without invoking any periodic structure assumptions, but only assuming the microstructure's statistics to be spatially homogeneous and ergodic. The SVE is set up on a mesoscale, i.e. any scale finite relative to the microstructural length scale. The Hill condition generalized to thermoelasticity dictates uniform Neumann and Dirichlet boundary conditions, which, with the help of two variational principles, lead to scale dependent hierarchies of mesoscale bounds on effective (RVE level) properties: thermal expansion and stress coefficients, effective stiffness, and specific heats. Due to the presence of a non-quadratic term in the energy formulas, the mesoscale bounds for the thermal expansion are more complicated than those for the stiffness tensor and the heat capacity. To quantitatively assess the scaling trend towards the RVE, the hierarchies are computed for a planar matrix-inclusion composite, with inclusions (of circular disk shape) located at points of a planar, hard-core Poisson point field. Overall, while the RVE is attained exactly on scales infinitely large relative to the microscale, depending on the microstructural parameters, the random fluctuations in the SVE response may become very weak on scales an order of magnitude larger than the microscale, thus already approximating the RVE.

1. **Introduction.** The problem of effective properties of material micro-structures has received considerable, and ever growing, attention over the past thirty years. By effective (or overall, macroscopic) is meant the constitutive response assuming the existence of a Representative Volume Element (RVE). In the case of spatial disorder having no microstructural periodicity, the RVE concept implies that there must be a scale (much) larger than the microscale (e.g., single heterogeneity size) to ensure a homogenization limit in the sense of Hill [1].

In general, the RVE is involved in the so-called

$$d < L \ll L_{macro} \tag{1.1}$$

2000 *Mathematics Subject Classification.* 35R60, 74F05, 74Q05, 74Q20, 74A60.

Key words and phrases. random media, thermoelasticity, homogenization, scale effects, representative volume element.

on which all of the deterministic continuum mechanics and physics hinges. Here, L is the RVE size, d is the microscale (average size of heterogeneity), and L_{macro} is the macroscale on which we set up, say, boundary value problems of elasticity theory. While the latter occurs for $L \ll L_{macro}$ (i.e. the range of continuum mechanics of homogeneous media), it is not clear what exactly is meant by $d < L$. Indeed, sometimes $d \ll L$ is implied. Without intending to sound critical, typical prescriptions of continuum solid mechanics vaguely state that domains roughly from 10 up to 100 times larger than the heterogeneity size should be taken, e.g. [2]. Overall, most studies of effective properties simply assume that the RVE is attained and do not specify or assess its size, e.g. [3-5].

Generally, the effective media studies usually follow one of four methods: (i) rigorous energy bounds (e.g., of Hashin-Shtrikman type), (ii) perturbation methods (e.g. [6]), (iii) effective medium models, and (iv) computational methods. Beginning with the late 1980s, we have seen the introduction of a fifth approach to determination of structure-property relations: bounds that explicitly involve (a) the size of a mesoscale domain relative to the microscale, and (b) the type of boundary conditions applied to this domain, e.g. [7-9]. That fifth approach was also driven by the need to derive continuum random field models of heterogeneous materials from actual microstructures [10,11].

Quantification of the tendency to asymptotically approach the RVE in the sense of Hill [1] as the size of the mesoscale domain increases - that domain also being called a Statistical Volume Element (SVE) - is of great practical interest. Random microstructures studied in the vein of the fifth approach mentioned above progressed from linear elastic to other types: physically and geometrically nonlinear elastic, viscoelastic, permeability phenomena, elastic-plastic and rigid-plastic; e.g. [12-17]. In general, the size of the RVE depends on several characteristics of microstructures, principal of which are: random microgeometries, mismatch in mechanical properties of individual phases, and the actual physics involved. The present research extends the above methodology to mesoscale bounds in a coupled field problem: thermal expansion coefficients, effective stiffness, and specific heat of linear thermoelastic microstructures; a short version was first given in [18].

Our analysis is based on variational principles of thermoelasticity, combined with the assumption of statistical homogeneity and ergodicity of the random medium, without any spatial periodicity assumptions. On that basis we derive hierarchies of scale-dependent tensors, bounding the RVE responses from above (and below) under uniform Dirichlet (respectively, uniform Neumann) boundary conditions. Using computational mechanics, we then quantitatively demonstrate the trend of these hierarchies to converge toward the RVE responses on the example of a two-phase random matrix-inclusion composite in two dimensions (2-D).

2. **Theoretical Fundamentals.**

2.1. **Random microstructure.** We take the random material to be a set $\mathcal{B} = \{B(\omega); \omega \in \Omega\}$ of realizations $B(\omega)$, defined over the sample space Ω. Thus, for an elementary event $\omega \in \Omega$, we have a realization $B(\omega)$, theoretically of infinite extent. From it we isolate an arbitrary mesoscale specimen $B_\delta(\omega)$, of finite size $L = \delta d$ and volume V_δ, bounded by a surface $S_\delta \equiv \partial V_\delta$, Fig. 1(a). Here we employ a non-dimensional *mesoscale* parameter defined as

$$\delta = \frac{L}{d}. \tag{2.1}$$

Ideally, $\delta \to \infty$ leads to homogeneous properties of heterogeneous materials. However, depending on the actual microstructural parameters, can be anything from a moderate to a very large number such that RVE is achieved within a required accuracy. It is the assessment of such a trend that is of interest to us here.

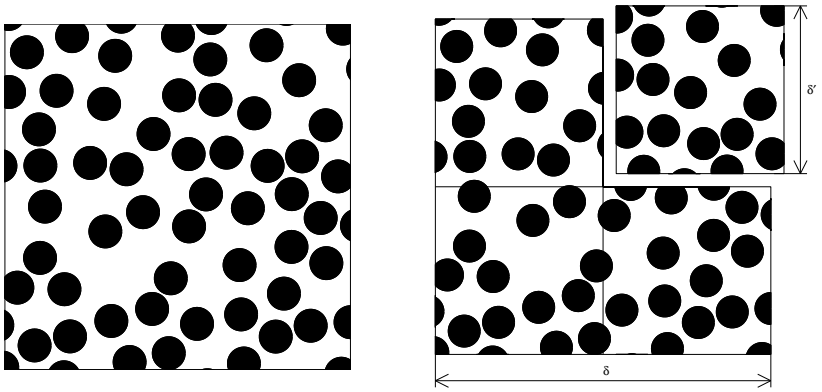

FIGURE 1. Planar model of a random composite material on a mesoscale δ, formed from a non-overlapping distribution of circular disks (Poisson hard-core process of disk centers); one deterministic configuration $B_\delta(\omega)$ at 40% nominal volume fraction of inclusions is shown. (b) Domain $B_\delta(\omega)$ of size $L(=\delta d)$, and its partitioning into four subdomains $B^s_{\delta'}(\omega)$ of size $L' = L/2$.

We require all the statistics of material properties to be spatially homogeneous and mean-ergodic. While the first property implies the invariance of all n-point distributions with respect to arbitrary shifts in spatial domain, the latter property means that the spatial average for any fixed realization $B(\omega)$ equals the ensemble average at any fixed point in the material domain

$$\overline{F(\omega)} \equiv \lim_{V\to\infty} \frac{1}{V}\int_V F(\omega,\mathbf{x})dV = \int_\Omega F(\omega,\mathbf{x})dP(\omega) \equiv \langle F(\mathbf{x})\rangle, \tag{2.2}$$

In (2.2) we introduce the overbar $\bar{\cdot}$ to denote a spatial average, and the brackets $\langle\cdot\rangle$ to denote an ensemble average; P is the probability distribution over Ω. More rigorous statements of the required ergodic properties of the material was given by Sab [8,9]. We assume the composite to be made of perfectly bonded phases, i.e. there are no displacement discontinuities.

2.2. **Constitutive laws in thermoelastic problems.** Locally (i.e. in each phase), the linear thermoelastic constitutive response is written as either

$$\varepsilon_{ij} = S_{ijkl}(\omega,\mathbf{x})\sigma_{kl} + \alpha_{ij}(\omega,\mathbf{x})\theta, \tag{2.3}$$

or

$$\sigma_{ij} = C_{ijkl}(\omega,\mathbf{x})\varepsilon_{kl} + \Gamma_{ij}(\omega,\mathbf{x})\theta, \tag{2.4}$$

where the thermal stress coefficient Γ_{ij} is linked to the thermal expansion coefficient α_{ij} by

$$\Gamma_{ij}(\omega,\mathbf{x}) = -C_{ijkl}(\omega,\mathbf{x})\alpha_{kl}(\omega,\mathbf{x}), \tag{2.5}$$

and θ $(= T - T_0)$ is a temperature change from the reference temperature T_0; $S_{ijkl}(\omega,\mathbf{x})$ and $C_{ijkl}(\omega,\mathbf{x})$ are the compliance and stiffness tensors, respectively.

[Hereafter we use the index and symbol notations for tensors interchangeably, as the need arises.]

At the microscale $\mathbf{C}$ is an inverse of $\mathbf{S}$, and a nice relation like (2.5) holds. However, when we go to the mesoscale $\delta > 1$, this reciprocity is no longer assured, and this topic will be discussed in Section 3 below. When we reach a medium homogenized at the level of of RVE ($\delta \to \infty$), the reciprocities are recovered [19], and we have

$$S^*_{ijkl} = C^{*-1}_{ijkl} \quad \Gamma^*_{ij} = -C^*_{ijkl}\alpha^*_{kl} \quad c^*_p - c^*_v = T_0 C^*_{ijkl}\alpha^*_{ij}\alpha^*_{kl}. \tag{2.6}$$

Hereafter, the superscript * indicates an effective property of a homogenized material (i.e. at the RVE, or macroscopic, level). The key question is: What mesoscale δ is needed to actually approximate the RVE level with a good accuracy?

2.3. **Energy formulations for heterogeneous materials.** In mechanics of elastic and inelastic heterogeneous materials, energetic approaches are widely used, especially when setting up variational principles used to bound the effective properties. Energy concepts appear also in the so-called Hill (or Hill-Mandel) condition [1] $\overline{\sigma} : \overline{\varepsilon} = \overline{\sigma : \varepsilon}$, which guarantees the equivalence of the mechanical and energetic approaches when determining the constitutive response, both at the macroscale and the mesoscale levels. Thus, if the stress and strain tensors are decomposed into their spatial average and fluctuating parts ($\sigma_{ij} = \overline{\sigma_{ij}} + \sigma'_{ij}$, $\varepsilon_{ij} = \overline{\varepsilon_{ij}} + \varepsilon'_{ij}$), the Hill condition is equivalent to a statement regarding the boundary values

$$\overline{\sigma : \varepsilon} = \overline{\sigma} : \overline{\varepsilon} \Longleftrightarrow \int_{\partial V_\delta} (\mathbf{t} - \overline{\sigma} \cdot \mathbf{n}) \cdot (\mathbf{u} - \overline{\varepsilon} \cdot \mathbf{x}) dS = 0. \tag{2.7}$$

This shows that, when the boundary conditions satisfy the right hand side above, the average of the product of the strain tensor and the stress tensor is equal to the product of their averages. For the sake of general reference, the derivation of (2.7) is given in the Appendix A.

With reference to the fundamentals of thermoelasticity theory, the Helmholtz free energy density A per unit volume at small temperature changes is

$$A = \frac{1}{2} C_{ijkl}\varepsilon_{ij}\varepsilon_{kl} + \Gamma_{ij}\varepsilon_{ij}\theta - \frac{1}{2} c_v \frac{\theta^2}{T_0}. \tag{2.8}$$

This gives stress and entropy

$$\sigma_{ij} = \left(\frac{\partial A}{\partial \varepsilon_{ij}}\right)_T \quad S = -\left(\frac{\partial A}{\partial T}\right)_{\varepsilon_{ij}}.$$

The potential energy is defined as

$$U^P = \frac{1}{V}\left(\int_{V_\delta} A dV - \int_{V_\delta} b_i u_i dV - \int_{S^t_\delta} t_i u_i dV\right), \tag{2.9}$$

where S^t_δ is the part of boundary S_δ with traction t_i prescribed on it, while b_i is the body force.

On the other hand, by a Legendre transformation, the Gibbs free energy is

$$G = -\frac{1}{2} S_{ijkl}\sigma_{ij}\sigma_{kl} - \alpha_{ij}\sigma_{ij}\theta - \frac{1}{2} c_p \frac{\theta^2}{T_0}, \tag{2.10}$$

and the constitutive laws are given by

$$\varepsilon_{ij} = -\left(\frac{\partial G}{\partial \sigma_{ij}}\right)_{T_0} \quad S = -\left(\frac{\partial G}{\partial T}\right)_{\sigma_{ij}}.$$

The complementary energy is defined as

$$U^C = -\frac{1}{V}\left(\int_{V_\delta} G dV + \int_{S_\delta^u} t_i u_i dV\right), \tag{2.11}$$

where S_δ^u is the part of S_δ with displacement u_i prescribed on it.

2.4. **Variational principles.** Again with reference to [19], we recall that the variational principles in a thermoelastic problem can be stated in terms of the potential and/or complementary energies. First, the variational principle in terms of the potential energy states that *of all the admissible displacement fields, those which satisfy the equilibrium equations make the potential energy minimum.* The minimum potential energy principle can be applied to a displacement controlled (or essential, Dirichlet) boundary value problem

$$U^{Pd} \leq \widetilde{U^{Pd}} \tag{2.12}$$

where $\widetilde{U^{Pd}}$ is calculated for an admissible strain field [20]. Here we insert the superscript 'd' on purpose so as to indicate the application of a displacement boundary condition.

The variational principle in terms of the complementary energy states that *of all the admissible stress fields, those which satisfy the compatibility equation of strain make the complementary energy minimum.* This can be applied to a traction controlled (or natural, Neumann) boundary value problem as follows

$$U^{Ct} \leq \widetilde{U^{Ct}} \tag{2.13}$$

where $\widetilde{U^{Ct}}$ denotes an admissible stress field, and 't' indicates a traction boundary condition.

Also, under the same kind of boundary condition, either traction or displacement, we have $U^{Pt} = -U^{Ct}$ or $U^{Pd} = -U^{Cd}$, respectively.

3. Mesoscale Bounds on Thermal Effects.

3.1. **Scale dependent hierarchy on the specific heat.** Under the hypothesis of spatially homogeneous and ergodic statistics of the material microstructure, we select an arbitrary realization $B_\delta(\omega)$ from $\mathcal{B}$. Henceforth, $B_\delta(\omega)$ is taken as a square-shaped mesoscale domain in 2-D, and a cubic-shaped one in 3-D. We next consider partitioning of $B_\delta(\omega)$ into 2^m subdomains ($m = 2$ and 3 in 2-D and 3-D, respectively), each subdomain $B_{\delta'}^s(\omega)$ being characterized by scale $\delta' = \delta/2$; $s = 1, 2, \ldots, 2^m$; see Fig. 1(b). Obviously,

$$B_\delta(\omega) = \cup_{s=1}^{2^m} B_{\delta'}^s(\omega) \tag{3.1}$$

First, under consideration are two uniform displacement boundary conditions consistent with $(2.7)_1$: one of an unrestricted type

$$u_i(\mathbf{x}) = \varepsilon_{ij}^0 x_j \qquad \forall \mathbf{x} \in \partial B_\delta, \tag{3.2}$$

and another of a restricted type applied to the partition (3.1)

$$u_i(\mathbf{x}) = \varepsilon_{ij}^0 x_j \quad \forall \mathbf{x} \in \partial B_{\delta'}^s, \quad s = 1, ..., 4. \tag{3.3}$$

The latter amounts to loading the entire domain B_δ both on its external boundary and on the internal cross partitioning B_δ into four subdomains $B_{\delta'}^s$. Given the perfect bonding throughout the material, $\varepsilon^0 = \bar{\varepsilon}$.

We now observe that the solution under the restricted condition (3.3) on all four subdomains $B^s_{\delta'}$ is an admissible solution with respect to the unrestricted condition (3.2) on B_δ, but not vice versa. Thus, in view of the principle of minimum potential energy, the following inequality is obtained

$$U^{Pd}_\delta \leq \sum_{s=1}^{4} U^{Pd}_{\delta'}(\omega) \tag{3.4}$$

The boundary condition (3.2) satisfies the Hill condition, so that, in view of (3.24) given below, (3.4) can be written as follows

$$\begin{aligned} &V_\delta \left(\frac{1}{2} C^d_{ijkl,\delta} \varepsilon^0_{ij} \varepsilon^0_{kl} + \Gamma^d_{ij,\delta} \varepsilon^0_{ij} \theta - \frac{1}{2} c^d_{v,\delta} \frac{\theta^2}{T_0} \right) \\ &\leq \sum_{s=1}^{4} V^s_{\delta'} \left(\frac{1}{2} C^{ds}_{ijkl,\delta'} \varepsilon^0_{ij} \varepsilon^0_{kl} + \Gamma^{ds}_{ij,\delta'} \varepsilon^0_{ij} \theta - \frac{1}{2} c^d_{v,\delta'} \frac{\theta^2}{T_0} \right). \end{aligned} \tag{3.5}$$

Here, and in the following, $C^d_{ijkl,\delta}$ and $C^{ds}_{ijkl,\delta'}$ are the apparent stiffness tensors for mesoscale domains B_δ and $B^s_{\delta'}$, respectively. [Thus, for example, $C^{ds}_{ijkl,\delta'}$ is subscript notation for the mesoscale tensor $\mathbf{C}^{ds}_{\delta'}$ in symbolic notation, with "$,\delta'$" indicating the mesoscale, not a partial differentiation.] These tensors are parametrized by a particular realization ω for a given $B(\omega)$, but we do not indicate that dependence for the sake of clarity. In the inequality (3.5) the elastic deformations and thermal effects are coupled. However, the case of zero temperature change θ reduces (3.5) to the well-known pure elasticity case $\langle \mathbf{C}^d_\delta \rangle \leq \langle \mathbf{C}^d_{\delta'} \rangle$. This then leads to a hierarchy of mesoscale stiffness tensors under displacement boundary conditions bounding the RVE response from above

$$\mathbf{C}^* \equiv \mathbf{C}^d_\infty \leq ... \leq \langle \mathbf{C}^d_\delta \rangle \leq \langle \mathbf{C}^d_{\delta'} \rangle \leq ... \leq \langle \mathbf{C}^d_1 \rangle \equiv \mathbf{C}^V \quad \forall \delta' = \delta/2, \tag{3.6}$$

where $\mathbf{C}^V$ is the Voigt bound. In view of (2.2), the ensemble averaging of $\mathbf{C}^d_\infty$ has been dropped.

On the other hand, setting the applied strain to zero ($\varepsilon^0_{ij} = 0$), leads to an inequality between ensemble averages on mesoscales δ and δ': $\langle c^d_{v,\delta} \rangle \geq \langle c^d_{v,\delta'} \rangle$. By extension to an arbitrary sequence of mesoscales, we arrive at the scale dependent hierarchy of volume specific heat at constant volume

$$c^*_v \equiv c^d_{v,\infty} \geq ... \geq \langle c^d_{v,\delta} \rangle \geq \langle c^d_{v,\delta'} \rangle \geq ... \geq c^d_{v,1} \equiv c^V_v \quad \forall \delta' = \delta/2, \tag{3.7}$$

where c^V_v is the Voigt bound.

We now turn to the reciprocal expression for the lower bound. We shall now load the mesoscale domain through either one of two types of uniform traction boundary conditions: one of an unrestricted type

$$t_i(\mathbf{x}) = \sigma^0_{ij} n_j \quad \forall \mathbf{x} \in \partial B_\delta, \tag{3.8}$$

and another of a restricted type applied to the partition (3.1)

$$t_i(\mathbf{x}) = \sigma^0_{ij} n_j \quad \forall \mathbf{x} \in \partial B^s_{\delta'}, \quad s = 1, ..., 4. \tag{3.9}$$

We note that $\sigma^0 = \overline{\sigma}$.

Considering the variational principle for complementary energy under both boundary conditions (3.8) and (3.9), an inequality similar to (3.4) can be obtained

$$U^{Ct}_\delta \leq \sum_{s=1}^{4} U^{Ct}_{\delta'}(\omega), \tag{3.10}$$

which, with reference to the Hill condition and (3.26), leads to

$$\begin{aligned} &V_\delta \left(\frac{1}{2} S^t_{ijkl,\delta} \sigma^0_{ij} \sigma^0_{kl} + \alpha^t_{ij,\delta} \sigma^0_{ij} \theta + \frac{1}{2} c^t_{p,\delta} \frac{\theta^2}{T_0} \right) \\ &\leq \sum_{s=1}^{4} V^s_{\delta'} \left(\frac{1}{2} S^t_{ijkl,\delta} \sigma^0_{ij} \sigma^0_{kl} + \alpha^t_{ij,\delta'} \sigma^0_{ij} \theta + \frac{1}{2} c^t_{p,\delta'} \frac{\theta^2}{T_0} \right). \end{aligned} \tag{3.11}$$

Again, for no thermal effects ($\theta = 0$), we arrive at the inequality $\langle \mathbf{S}^t_\delta \rangle \leq \langle \mathbf{S}^t_{\delta'} \rangle$, under the traction boundary condition, which leads to a well-known scale dependent hierarchy on the effective (RVE level) compliance tensor

$$\mathbf{S}^* \equiv \mathbf{S}^t_\infty \leq ... \leq \langle \mathbf{S}^t_\delta \rangle \leq \langle \mathbf{S}^t_{\delta'} \rangle \leq ... \leq \langle \mathbf{S}^t_1 \rangle \equiv \mathbf{S}^R \quad \forall \delta' = \delta/2. \tag{3.12}$$

where $\mathbf{S}^R$ is the Reuss bound, and the same remark as that following (3.6) applies.

On the other hand, when $\sigma^0_{ij} = 0$, we obtain an inequality between ensemble averages on mesoscales δ and δ': $\langle c^t_{p,\delta} \rangle \leq \langle c^t_{p,\delta'} \rangle$. Again by extension to an arbitrary sequence of mesoscales, this leads to the scale dependent hierarchy of pressure specific heat under the traction boundary condition as follows

$$c^*_p \equiv c^t_{p,\infty} \leq ... \leq \langle c^t_{p,\delta} \rangle \leq \langle c^t_{p,\delta'} \rangle \leq ... \leq c^t_{p,1} \equiv c^V_p \quad \forall \delta' = \delta/2. \tag{3.13}$$

This is the hierarchy of upper bounds on the pressure specific heat under the traction boundary condition (3.8). According to the hierarchies (3.11) and (3.12), we can see that the constitutive relation $(2.6)_3$ does not hold unless the domain size reaches the RVE size. Thus, combining (2.6), (3.7) and (3.13) we obtain a hierarchy including both upper and lower bounds:

$$\begin{aligned} &\langle c^t_{p,1} \rangle - \langle T_0 C^t_{ijkl,1} \alpha^t_{ij,1} \alpha^t_{kl,1} \rangle \geq ... \geq \langle c^t_{p,\delta'} \rangle - \langle T_0 C^t_{ijkl,\delta'} \alpha^t_{ij,\delta'} \alpha^t_{kl,\delta'} \rangle \\ &\geq \langle c^t_{p,\delta} \rangle - \langle T_0 C^t_{ijkl,\delta} \alpha^t_{ij,\delta} \alpha^t_{kl,\delta} \rangle \geq ... \geq \langle c^*_p \rangle - \langle T_0 C^*_{ijkl} \alpha^*_{ij} \alpha^*_{kl} \rangle \\ &\geq c^*_v \geq ... \geq \langle c^d_{v,\delta} \rangle \geq \langle c^d_{v,\delta'} \rangle \geq ... \geq c^d_{v,1} \quad \forall \delta' = \delta/2. \end{aligned} \tag{3.14}$$

where $C^t_{ijkl,1} = (S^t_{ijkl,1})^{-1}$. This hierarchy shows the upper and lower bound character on the effective specific heat and the scaling trend to RVE of both mesoscale bounds. In Section 4 a numerical simulation quantitatively demonstrates the convergence trends.

3.2. **Scale effects on the thermal expansion coefficient.** We now turn to scale dependent hierarchical bounds on effective thermal expansion coefficients. This case is different from that of the stiffness and compliance tensors as well as the specific heat capacities under constant pressure/displacement because of the presence of a non-quadratic term in both energy formulations (2.8) and (2.10). Clearly, this term couples the elastic and thermal effects. Therefore, the hierarchical bounds on thermal expansion coefficients do not simply mimic the upper/lower bounds on stiffness and compliance tensors under displacement/traction boundary conditions. However, we may use the latter to obtain the former.

We now consider a two-phase composite material with properties of phase 1 being $C^{(1)}_{ijkl}, \alpha^{(1)}_{ij}, ...$ and those of phase 2 being $C^{(2)}_{ijkl}, \alpha^{(2)}_{ij}, ...$. It was shown earlier by Christensen [19] that, under the traction boundary condition (3.8) and by setting $P_{klmn}(S^t_{mnij} - S^{(2)}_{mnij}) = I_{klij}$, the thermal expansion coefficient can be expressed as

$$\alpha^t_{ij} = (\alpha^{(1)}_{kl} - \alpha^{(2)}_{kl}) P_{klmn} (S^t_{mnij} - S^{(2)}_{mnij}) + \alpha^{(2)}_{ij}. \tag{3.15}$$

Similarly, under the displacement boundary condition (3.2), and by setting $P_{klmn}(S^{(1)}_{mnij}–S^{(2)}_{mnij}) = I_{klij}$, for the thermal stress coefficient we have

$$\Gamma^d_{ij} = (\Gamma^{(1)}_{kl} - \Gamma^{(2)}_{kl})P_{klmn}(C^d_{mnij} - C^{(2)}_{mnij}) + \Gamma^{(2)}_{ij}. \tag{3.16}$$

From the scale dependence of compliance and stiffness tensors (S^t_{mnij} and C^d_{mnij}) we can next derive the scale dependence of thermal expansion coefficients since P_{klmn} is scale independent by definition. Thus, considering each phase to be isotropic and macroscopically isotropic, from (3.15) we have a simplified relation

$$\alpha^t_{ij} = (\alpha^{(1)} - \alpha^{(2)})\frac{S^t_{nnij} - \delta_{ij}/\kappa^{(2)}}{1/\kappa^{(1)} - 1/\kappa^{(2)}} + \alpha^{(2)}\delta_{ij}, \tag{3.17}$$

where S^t_{mnij} is the mesoscale compliance tensor under traction boundary condition, and $\kappa^{(1)}$ denotes the bulk modulus of phase 2. Next, taking an ensemble average over (3.17), and noting the scale dependent hierarchy (3.12), leads to two scale dependent hierarchies for the isotropic part α^t_δ of $\alpha^t_{ij,\delta}$:

(i) $\alpha^{(1)} \geq \alpha^{(2)} \geq 0$ and $\kappa^{(1)} > \kappa^{(2)}$:

$$\alpha^* \geq ... \geq \langle\alpha^t_\delta\rangle \geq \langle\alpha^t_{\delta'}\rangle \geq ... \geq \alpha^t_1 \equiv \alpha^R \quad \forall\delta' = \delta/2. \tag{3.18}$$

(ii) $\alpha^{(1)} \geq \alpha^{(2)} \geq 0$ and $\kappa^{(1)} < \kappa^{(2)}$:

$$\alpha^* \leq ... \leq \langle\alpha^t_\delta\rangle \leq \langle\alpha^t_{\delta'}\rangle \leq ... \leq \alpha^t_1 \equiv \alpha^V \quad \forall\delta' = \delta/2. \tag{3.19}$$

where α^R is the Reuss-type bound on α^*.

Using an expression for Γ^d_{ij} entirely analogous to (3.17), we find

$$\Gamma^d_{ij} = (\Gamma^{(1)} - \Gamma^{(2)})\frac{C^d_{nnij} - \delta_{ij}\kappa^{(2)}}{\kappa^{(1)} - \kappa^{(2)}} - \Gamma^{(2)}\delta_{ij}. \tag{3.20}$$

With the help of (3.6) we derive two hierarchical relations for the isotropic part Γ^d_δ of $\Gamma^d_{ij,\delta}$:

(i) $0 \geq \Gamma^{(1)} \geq \Gamma^{(2)} \geq 0$ and $\kappa^{(1)} > \kappa^{(2)}$:

$$\Gamma^* \leq ... \leq \langle\Gamma^d_\delta\rangle \leq \langle\Gamma^d_{\delta'}\rangle \leq ... \leq \Gamma^d_1 \equiv \Gamma^V \quad \forall\delta' = \delta/2. \tag{3.21}$$

(ii) $0 \geq \Gamma^{(1)} \geq \Gamma^{(2)} \geq 0$ and $\kappa^{(1)} < \kappa^{(2)}$:

$$\Gamma^* \geq ... \geq \langle\Gamma^d_\delta\rangle \geq \langle\Gamma^d_{\delta'}\rangle \geq ... \geq \Gamma^d_1 \equiv \Gamma^V \quad \forall\delta' = \delta/2. \tag{3.22}$$

where Γ^V is the Voigt-type bound on Γ^*.

A closer inspection reveals that taking the special case $\kappa^{(1)} = \kappa^{(2)}$ does not present a singularity in (3.18-19) and (3.21-22). Note that, since the Hill condition is satisfied on any mesoscale with either (3.2) or (3.8), we can use apparent properties in the constitutive relation $(2.6)_2$ so as to arrive at upper and lower mesoscale bounds and scaling towards the RVE. The numerical simulation results of Section 4 demonstrate the aforementioned bounds.

3.3. **Legendre transformations.** For a homogeneous continuum – or also (as mentioned at the end of Section 2.2) for a material homogenized at the RVE level - the complementary energy under a prescribed traction boundary condition and the potential energy under a prescribed displacement boundary condition are the negative of each other

$$U^P = -U^C \tag{3.23}$$

We also have this classical Legendre transformation linking the Helmholtz and Gibbs energies

$$A(\varepsilon_{ij},\theta) = G(\sigma_{ij},\theta) + \sigma_{ij}\varepsilon_{ij}. \tag{3.24}$$

Here we simply write A, G, σ_{ij} and ε_{ij}. This, of course, is one pair out of all four possible Legendre transformations in a quartet linking the internal energy, Helmholtz free energy, enthalpy, and Gibbs energy when the temperature (θ) and entropy (s) are kept as passive variables, e.g. [20]. In a random medium (i.e., at the SVE level below the RVE), the quartet must be interpreted carefully according as either displacement or traction boundary conditions are applied. Following [21], we examine these possibilities.

First, assuming loading via (3.2), we must consider the spatial fluctuation terms and thus, we write the Helmholtz and Gibbs energies in the following forms

$$A_\delta(\varepsilon^0_{ij},\theta,\omega) = \frac{1}{2}C_{ijkl,\delta}(\omega)\varepsilon^0_{ij}\varepsilon^0_{kl} + \Gamma_{ij,\delta}(\omega)\varepsilon^0_{ij}\theta - \frac{1}{2}c_{v,\delta}(\omega)\frac{\theta^2}{T_0}, \tag{3.25}$$

and

$$G_\delta(\sigma^0_{ij},\theta,\omega) = -\frac{1}{2}S_{ijkl,\delta}(\omega)\sigma^0_{ij}\sigma^0_{kl} - \alpha_{ij,\delta}(\omega)\sigma_{ij}\theta - \frac{1}{2}c_{p,\delta}(\omega)\frac{\theta^2}{T_0}. \tag{3.26}$$

Upon ensemble averaging, (3.25-26) become

$$\langle A_\delta(\varepsilon^0_{ij},\theta)\rangle = \frac{1}{2}\langle C_{ijkl,\delta}\rangle\varepsilon^0_{ij}\varepsilon^0_{kl} + \langle\Gamma_{ij,\delta}\rangle\varepsilon^0_{ij}\theta - \frac{1}{2}\langle c_{v,\delta}\rangle\frac{\theta^2}{T_0}, \tag{3.27}$$

and

$$\langle G_\delta(\sigma^0_{ij},\theta)\rangle = -\frac{1}{2}\langle S_{ijkl,\delta}\rangle\sigma^0_{ij}\sigma^0_{kl} - \langle\alpha_{ij,\delta}\rangle\sigma^0_{ij}\theta - \frac{1}{2}\langle c_{p,\delta}\rangle\frac{\theta^2}{T_0}. \tag{3.28}$$

It follows that, under displacement boundary conditions (ε^0_{ij} controlled), the volume average stress is random (i.e., $\overline{\sigma_{ij}(\omega)}$), so that

$$G_\delta(\overline{\sigma_{ij}(\omega)},\theta) = A_\delta(\varepsilon^0_{ij},\theta,\omega) - \overline{\sigma_{ij}(\omega)}\varepsilon^0_{ij}, \tag{3.29}$$

and hence, the ensemble average Gibbs energy on mesoscale δ should be calculated from $\langle A_\delta(\varepsilon^0_{ij},\theta)\rangle$ according to

$$G_\delta(\langle\overline{\sigma_{ij}}\rangle,\theta) = \langle A_\delta(\varepsilon^0_{ij},\theta)\rangle - \langle\overline{\sigma_{ij}}\rangle\varepsilon^0_{ij}, \tag{3.30}$$

rather than as $\langle G_\delta(\overline{\sigma_{ij}(\omega)},\theta)\rangle$.

Similarly, under traction boundary conditions (σ^0_{ij} controlled), the volume average strain is random (i.e., $\varepsilon^0_{ij}(\omega)$), so that

$$A_\delta(\overline{\varepsilon_{ij}(\omega)},\theta) = G_\delta(\sigma^0_{ij},\theta,\omega) + \sigma^0_{ij}\overline{\varepsilon_{ij}(\omega)}, \tag{3.31}$$

and hence, the ensemble average Helmholtz energy on mesoscale δ should be calculated from according to

$$\langle A_\delta(\overline{\varepsilon_{ij}},\theta)\rangle = \langle G_\delta(\sigma^0_{ij},\theta)\rangle + \sigma^0_{ij}\langle\overline{\varepsilon_{ij}}\rangle, \tag{3.32}$$

rather than as $\langle A_\delta(\overline{\varepsilon_{ij}(\omega)},\theta)\rangle$. When the mesoscale SVE reaches the RVE, the dependence on the type of boundary conditions vanishes, and we recover the classical relation (3.24) for a homogeneous material.

4. **Numerical Simulations of Scaling Trends.**

4.1. **Methodology.** In order to demonstrate the hierarchies of bounds derived in Section 3, a series of numerical simulation is carried out on different mesoscales and under different boundary conditions. Our attention is focused on a 2-D, two-phase matrix-inclusion composite material with circular shaped inclusions, everywhere perfectly bonded. A finite element mesh, finer than the single inclusion, is employed. The inclusion and matrix phases have different Young's moduli E, Poisson ratios ν, thermal expansion coefficients α and specific heats c_p. In general, this leads to a characterization of the composite in terms of four mismatches (contrasts, or ratios of the inclusion property to the matrix property): E^i/E^m, ν^i/ν^m, α^i/α^m, and c_p^i/c_p^m. Each realization is generated by a hard-core Poisson point field (Fig. 1(a)), with the inter-point distance being 1.2 times the disk diameter (so as to avoid the special problem of very narrow necks between the inclusions), and this process is repeated in a Monte Carlo sense to simulate an ensemble. The material properties and mismatches are listed in Table 1. Perfect bonding between the inclusion and matrix phases is assumed.

	$E\ [GPa]$	ν	$\alpha\ [1/K]$	$c_p^i\ [Jg/K]$
Aluminum matrix (phase 1)	71	0.3	2.4 10^{-5}	0.900
Steel inclusions (phase 2)	211	0.3	1.2 10^{-5}	0.452
Mismatches	3	1	0.5	0.5

TABLE 1. Material properties of steel and aluminum

δ	2	4	8	16	32
number of specimens $B_\delta(\omega)$	160	81	49	32	16

TABLE 2. Number of specimens in the Monte Carlo simulation; increasing the numbers of the second row had no noticeable effects on the averages.

To compute all the hierarchies of Section 3, we proceed in the following steps:

(a) Choose a specific mesoscale δ and a nominal disk volume fraction;

(b) Generate a mesoscale realization $B_\delta(\omega)$ of the disordered medium;

(c) For a specific $B_\delta(\omega)$, compute the stiffness tensor $\mathbf{C}_\delta^d(\omega)$, the thermal expansion stress coefficient $\mathbf{\Gamma}_\delta^d(\omega)$ and the constant-volume specific heat $c_{v,\delta}(\omega)$ numerically, Fig. 2. $\mathbf{C}_\delta^d(\omega)$ is computed under a non-zero displacement boundary condition (3.2) using various settings of ε_{ij}^0; $\mathbf{\Gamma}_\delta^d(\omega)$ and $c_{v,\delta}(\omega)$ are computed under $\varepsilon_{ij}^0 = 0$ and the temperature change $\theta = 5K$ up from $T_0 = 293.15K$. Then, ensemble averages are taken to compute mesoscale bounds on the given mesoscale δ.

(d) For the same $B_\delta(\omega)$, compute the compliance tensor $\mathbf{S}_\delta^t(\omega)$, the thermal expansion strain coefficient $\alpha_\delta^t(\omega)$ and the constant-pressure specific heat $c_{p,\delta}(\omega)$ numerically, Fig. 2. $\mathbf{S}_\delta^t(\omega)$ is computed under a non-zero traction boundary condition (3.8), using various settings of σ_{ij}^0; $\alpha_\delta^t(\omega)$ and $c_{p,\delta}(\omega)$ are computed under $\sigma_{ij}^0 = 0$ and the temperature change $\theta = 5K$ up from $T_0 = 293.15K$.

(e) Proceed from (a) to (d) in a Monte Carlo sense over the sample space Ω, according to the Table 2, so as to generate an ensemble of results at a fixed mesoscale δ : $\{\mathbf{C}_\delta^d(\omega), \mathbf{\Gamma}_\delta^d(\omega), c_{v,\delta}^d(\omega); \omega \in \Omega\}$ and $\{\mathbf{S}_\delta^d(\omega), \alpha_\delta^d(\omega), c_{p,\delta}^t(\omega); \omega \in \Omega\}$. Then, ensemble averages are taken to compute mesoscale bounds on the given mesoscale δ.

(f) Change the mesoscale and repeat steps (a) to (e). We then compute the first moments in function of δ (i.e. scale dependent bounds) for all the mesoscale properties. Of course, higher moments may also be computed in the same fashion.

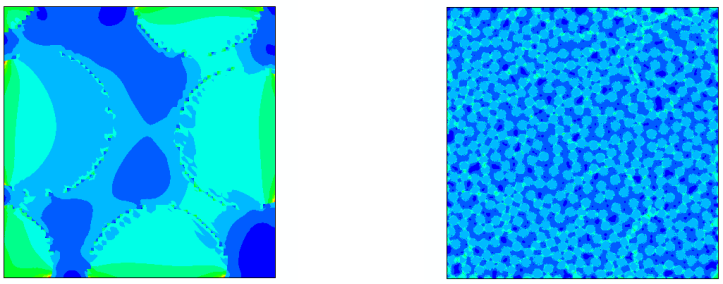

FIGURE 2. Numerical results on $\varepsilon = 2$ and $\varepsilon = 32$ under the displacement boundary condition (3.2) at ε^0_{ij}; disks do not touch.

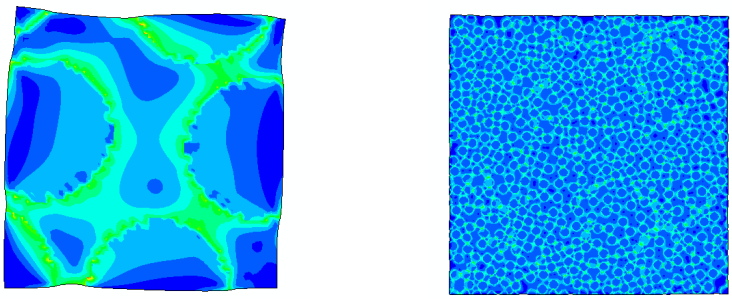

FIGURE 3. Numerical results on $\delta = 2$ and $\delta = 32$ under the traction boundary condition (3.8) at σ^0_{ij}; disks do not touch.

Figures 2 and 3 demonstrate sample results on a very small mesoscale and a rather large mesoscale. In Fig. 3(a) for $\delta = 2$, the boundary deformation is very pronounced. On the other hand, for $\delta = 32$ in Fig. 3(b), the boundary deformation is hardly seen. This illustrates the scaling trend from SVE towards the RVE. Since we deal with infinitesimal strains in linear thermoelasticity, in order to visualize the differences between responses under displacement versus traction boundary conditions, displacements in these figures are plotted with an amplification factor of 200.

4.2. **Numerical results.**

4.2.1. *Scaling of specific heats c_v and c_p.* The hierarchy (3.7) states that the ensemble average of the specific heat c_v under constant volume increases when the mesoscale δ increases. This is brought out in Fig. 4(a). On the other hand, Fig 4(b) confirms that the ensemble average of c_p decreases with increasing δ. All these results are combined in Fig. 5, where we use the notation $c^t_v = c^t_p - T_0 C^*_{ijkl}\alpha^*_{ij}\alpha^*_{kl}$. For rather small mismatches in material properties chosen here, the numerical differences between $\langle c^d_{v,\delta}\rangle$ and $\langle c^t_{p,\delta}\rangle$ are (very) small, but the methodology developed here can be applied to study higher contrast materials.

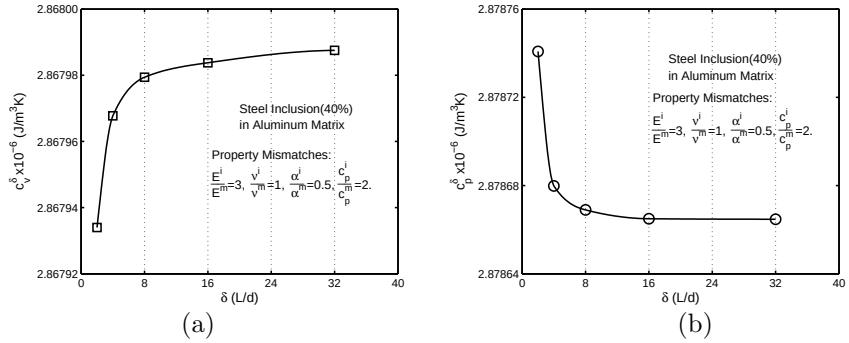

FIGURE 4. Hierarchical trends for: (a) c_v^d under displacement boundary condition; (b) c_p^t under traction boundary condition.

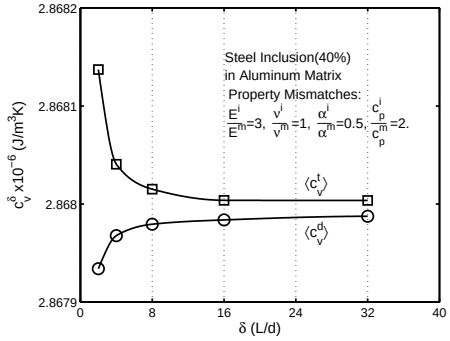

FIGURE 5. Scaling of specific heat capacities from SVE towards RVE; the same results were shown separately in Fig. 4.

4.2.2. *Scaling of thermal expansion coefficients.* Thermal expansion coefficients are also scale dependent due to their relation with the elastic properties stated in (3.15) and (3.16). We henceforth carry out numerical simulation to exhibit their scale dependent trends as per (3.18-17) and (3.21-22). Figure 6 shows the results. With reference to Table 1, we see that $\alpha^{(1)} > \alpha^{(2)} \geq 0$ and $\kappa^{(1)} < \kappa^{(2)}$ so that the scale dependence trend of $\langle \alpha_{ij}^t \rangle$ follows the hierarchy (3.19): it decreases with δ increasing. On the other hand, considering the displacement boundary condition, the composite material model has the mismatches $0 \geq \Gamma^{(1)} > \alpha^{(1)} > \alpha^{(2)} \geq 0$ and $\kappa^{(1)} > \kappa^{(2)}$. Therefore, the scale dependent trend of $\langle \Gamma_{ij}^d \rangle$ must follow the hierarchy (3.21). Figure 6(b) shows that the trace of $\langle \Gamma_{ij}^d \rangle$ increases with increasing δ.

In order to obtain the convergence of $\langle \Gamma_{ij}^d \rangle$ and $\langle \alpha_{ij}^t \rangle$ towards the RVE, two separate hierarchical trends may not be sufficient to assess the size of RVE - both (upper and lower) mesoscale bounds are jointly necessary. Thus, we can apply equation (2.5) to set up bounds (upper and lower) in terms of displacement and traction boundary conditions. Figure 6(c) shows numerical result on the upper and lower bounds for the trace of the stiffness tensor under displacement and traction boundary conditions. Consequently, modifying the formula (2.5) to $\Gamma_{kl}^t = -C_{klij}^t \alpha_{ij}^t$, and using the Legendre transformations of Section 3.3, the thermal stress coefficient corresponding to the traction boundary condition is obtained at any given mesoscale.

Figure 6(d) shows that both thermal stress coefficients under displacement and traction boundary conditions converge toward each other as $\delta \to \infty$. At $\delta = 32$, the difference between Γ^d_{ij} and Γ^t_{ij} is less than 0.2%. Thus, $\delta = 32$ may be adopted as the RVE scale, the actual choice of that difference being, of course, a matter of taste.

As stated in the derivation of (3.18-19) and (3.21-22), different mismatches in composites may present different hierarchical trends. We therefore complete this paper with a study of two different kinds of composites having these mismatches:

composite #1: $\dfrac{E^i}{E^m} = 3,\ \dfrac{\nu^i}{\nu^m} = 1,\ \dfrac{\alpha^i}{\alpha^m} = 2;$

composite #2: $\dfrac{E^i}{E^m} = 3,\ \dfrac{\nu^i}{\nu^m} = 1,\ \dfrac{\alpha^i}{\alpha^m} = 0.2.$

In Fig. 7, these two 'opposite' cases of mismatches are compared. In particular, Fig. 7(a) shows that the composite displays a hierarchical trend of $\langle \alpha^t_{ij} \rangle$ according to (3.18), while Fig. 7(b) presents the trend according to (3.19). Furthermore, Fig. 7(c) shows that $\langle \Gamma^d_{ij} \rangle$ increases with the increase of δ, as given in (3.22). With different mismatches of materials, Fig 7(d) shows the trend stated in (3.21). Once again, employing the Legendre transformations of Section 3.3, we compute the upper and lower bounds presented in Figs. 7(e) and (f). In the case of the composite #1, the traction boundary condition provides the upper bound, while the displacement boundary condition provides the lower bound. In contradistinction to this, in the case of the composite #2, the traction boundary condition gives the lower bound while the displacement boundary condition gives the upper bound. In both cases, we clearly see that both bounds converge toward each other with the mesoscale increasing.

5. **Conclusions.** Results of this paper may be summarized as follows:

i) The Hill condition is employed so as to develop the equivalence between the energetic and mechanical formulations of constitutive laws of thermoelastic random heterogeneous materials at arbitrary mesoscale.

ii) Using the potential and complementary energy principles, we obtain scale dependent hierarchies for the upper and lower bounds on the specific heat capacity at the RVE level. Application of displacement (respectively, traction) boundary condition results in a hierarchy of lower bounds on c^d_v (upper bounds on c^t_p). With the increasing mesoscale, both bounds converge to one another in the sense that $c^*_p - c^*_v = T_0 C^*_{ijkl} \alpha^*_{ij} \alpha^*_{kl}$ is attained.

iii) Due to the presence of a non-quadratic term in the energy formulas, the mesoscale bounds on the thermal expansion are more complicated than those on the stiffness tensor and the heat capacity. In general, the upper and lower bounds correspond to loading of mesoscale domains by displacement and traction boundary conditions. Depending on the property mismatches, the upper and lower bounds can be provided either by displacement boundary condition or traction boundary conditions.

iv) In the proposed scale-dependent homogenization of thermoelastic properties, the RVE properties are attained approximately on a finite scale with whatever desired accuracy. In other words, the condition $d \ll L$ in the separation of scales (1.1) is not always necessary, and it is possible that the RVE is attained simply at $d < L$, i.e., only an order of magnitude smaller than L.

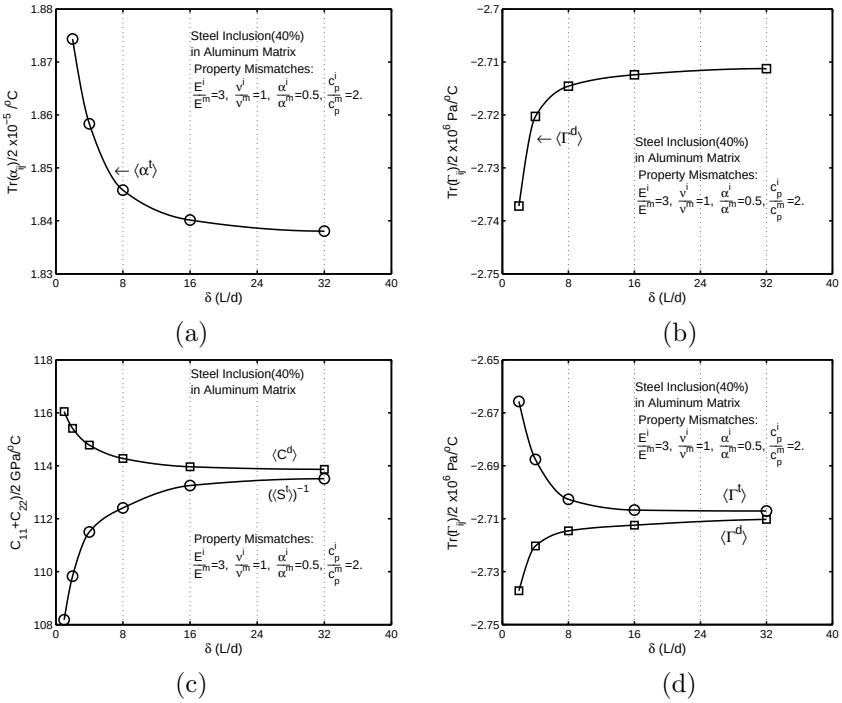

FIGURE 6. Numerical results for the aluminum-steel composite of Fig. 1. (a) scale effect on thermal strain coefficient under zero traction boundary condition; (b) scale effect on thermal stress coefficient under zero displacement boundary condition; (c) mesoscale bounds (upper and lower) on stiffness; (d) mesoscale bounds (upper and lower) on thermal stress coefficient.

Appendix A. **The Hill conditon.** The Hill condition $(2.7)_1$ is a prerequisite for setting up the equivalence between the mechanical and energetic approaches to constitutive laws. In elasticity, along with the average strain/stress theorems, it provides a foundation for mesoscale bounds on effective moduli of heterogeneous materials. To derive the Hill condition one starts from the observation that, for any volume V, the difference between the volume average of strain energy and the strain energy calculated from the volume average strss and strain fields (where we drop the factor 1/2 for simplicity) is

$$\overline{\sigma_{ij}\varepsilon_{ij}} - \overline{\sigma_{ij}}\ \overline{\varepsilon_{ij}} = \overline{\sigma'_{ij}\varepsilon'_{ij}} \tag{A.1}$$

In (A.1) σ'_{ij} and ε'_{ij} are the fluctuations in stress and strain fields, respectively. Next, noting that $\varepsilon_{ij} = u_{(i,j)}$, we have

$$\begin{aligned}
\overline{\sigma'_{ij}\varepsilon'_{ij}} &= \frac{1}{V}\int_V (\sigma_{ij} - \overline{\sigma_{ij}})(\varepsilon_{ij} - \overline{\varepsilon_{ij}})dV \\
&= \frac{1}{V}\int_V \left\{ \left[(\sigma_{ij} - \overline{\sigma_{ij}})(u_i - \overline{u_i})\right]_{,j} - (\sigma_{ij,j} - \overline{\sigma_{ij,j}})(u_i - \overline{u_i}) \right\} dV \\
&= \frac{1}{V}\int_{\partial V} \left[(\sigma_{ij} - \overline{\sigma_{ij}})(u_i - \overline{u_i})\right] n_j dS \\
&= \frac{1}{V}\int_{\partial V} \left[(t_i - \overline{\sigma_{ij}}n_j)(u_i - \overline{\varepsilon_{ij}}x_j)\right] dS.
\end{aligned} \tag{A.2}$$

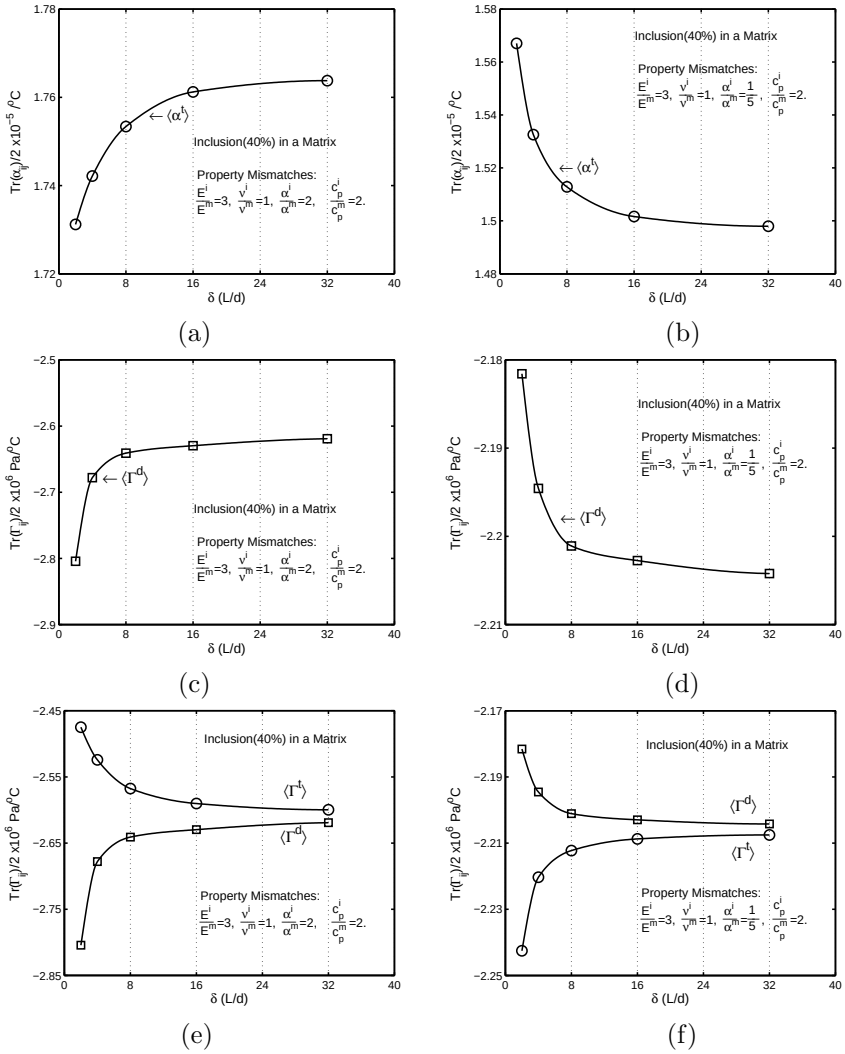

FIGURE 7. Hierarchies of upper and lower bounds for two composite models (#1 and #2) of Section 4.2.2: (a) and (b) scale effects on thermal strain coefficients under zero traction boundary condition; (c) and (d) scale effects on thermal stress coefficients under zero displacement boundary condition; (e) and (f) mesoscale bounds (upper and lower) on thermal stress coefficients.

In (A.2) the second line follows from the integration by parts. Next, the second term in the the second part of the integrand may be dropped assuming the absence of body and inertia forces. The third line follows from the Green-Gauss theorem, and the fourth from the Cauchy's stress concept and the property of affine displacement fields.

Acknowledgements. The work reported herein has been made possible through support by the NSERC and the Canada Research Chairs program.

REFERENCES

[1] Hill, R. (1963), Elastic properties of reinforced solids: Some theoretical principles. *J. Mech. Phys. Solids* **11**, 357-372.

[2] Lemaitre, J. & Chaboche, J.-L. (1994), *Mechanics of Solid Materials*, Cambridge University Press.

[3] Markov, K.Z. & Preziosi, L. (2000), *Heterogeneous Media*, Birkhäuser, Basel.

[4] Nemat-Nasser, S. & Hori, M. (1993), *Micromechanics: Overall Properties of Heterogeneous Solids*, North-Holland, Amsterdam.

[5] Torquato, S. (2002), *Random Heterogeneous Materials: Microstructure and Macroscopic Properties*, Springer-Verlag, Berlin-New York.

[6] Beran, M.J. (1968), *Statistical Continuum Theories*, J. Wiley & Sons.

[7] Huet, C., (1990), Application of variational concepts to size effects in elastic heterogeneous bodies, *J. Mech. Phys. Solids* **38**, 813-841.

[8] Sab, K. (1992), On the homogenization and simulation of random materials, *Eur. J. Mech. A/Solids* **11**(5), 585-607.

[9] Sab, K. (1991), Principe de Hill et homogénéisation des matériaux aléatoires, *C. R. Acad. Sci. Paris II* **312**, 1-5.

[10] Ostoja-Starzewski, M. & Wang, C. (1989), Linear elasticity of planar Delaunay networks: Random field characterization of effective moduli, *Acta Mech.* **80**, 61-80.

[11] Ostoja-Starzewski, M. (1994) Micromechanics as a basis of continuum random fields, *Appl. Mech. Rev.* (Special Issue: *Micromechanics of Random Media*) **47**(1, Part 2), S221-S230.

[12] Hazanov, S. (1998), On apparent properties of nonlinear heterogeneous bodies smaller than the representative volume, *Acta Mech.* **134**, 123-134.

[13] Huet, C. (1999), Coupled size and boundary-condition effects in viscoelastic heterogeneous and composite bodies, *Mech. Mater.* **31**(12), 787-829.

[14] Khisaeva, Z.F. & Ostoja-Starzewski, M. (2006), Mesoscale bounds in finite elasticity and thermoelasticity of random composites, *Proc. R. Soc. Lond. A* **462**, 1167 - 1180.

[15] Ostoja-Starzewski, M. (2001), Mechanics of random materials: Stochastics, scale effects, and computation, in *Mechanics of Random and Multiscale Microstructures* (Eds. D. Jeulin & M. Ostoja-Starzewski), *CISM Courses and Lectures* **430**, Springer-Wien-New York, 93-161.

[16] Ostoja-Starzewski, M. (2005), Scale effects in plasticity of random media: Status and challenges, *Int. J. Plast.* **21**, 1119-1160.

[17] Du, X & Ostoja-Starzewski, M. (2006), On the size of representative volume element for Darcy law in random media, *Proc. R. Soc. Lond. A*, in press.

[18] Du, X. & Ostoja-Starzewski, M. (2005), Mesoscale bounds on effective thermal expansion of random composites, *Proc. 20th CANCAM*, 463-464, Montréal, Canada.

[19] Christensen, R.M. (1979), *Mechanics of Composite Materials*, J. Wiley & Sons.

[20] Houlsby, G.T. & Puzrin, A.M. (2000), Application of thermomechanical principles to the modelling of geotechnical materials. *Int. J. Plast.* **16**, 1017-1047.

[21] Ostoja-Starzewski, M. (2002), Towards stochastic continuum thermodynamics, *J. Non-Equilib. Thermodyn.* **27**(4), 335-348.

Received November 2005; revised February 2006.

E-mail address: xdu1@po-box.mcgill.ca
E-mail address: martinos@uiuc.edu